**ELSEVIER**

# Atmospheric correction of MODIS data in the visible to middle infrared: first results

Eric F. Vermote [a],*, Nazmi Z. El Saleous [b], Christopher O. Justice [a]

[a]*Department of Geography, University of Maryland, NASA Goddard Space Flight Center, Code 923, Greenbelt, MD 20771, USA*
[b]*Raytheon ITSS, USA*

## Abstract

The MODIS instrument provides major advances in moderate resolution earth observation. Improved spatial resolution for land observation at 250 and 500 m and improved spectral band placement provide new remote sensing opportunities. NASA has invested in the development of improved algorithms for MODIS, which will provide new data sets for global change research. Surface reflectance is one of the key products from MODIS and is used in developing several higher-order land products. The surface reflectance algorithm builds on the heritage of the Advanced Very High Resolution Radiometer (AVHRR) and SeaWiFS algorithms, taking advantage of the new sensing capabilities of MODIS. Atmospheric correction by the removal of water vapor and aerosol effects provides improvements over previous coarse resolution products and the basis for a new time-series, which will extend through to the NPOESS generation imagers. This paper summarizes the first evaluation of the MODIS surface reflectance product accuracy, in comparison with other data products and in the context of the MODIS instrument performance since launch. The MODIS surface reflectance product will provide an important time-series data set for quantifying global environmental change.
© 2002 Elsevier Science Inc. All rights reserved.

## 1. Introduction

Remote sensing in the visible to middle infrared spectrum provides some of the key inputs for understanding the biosphere and its dynamics. Since the 1980s, red and near-infrared data from the Advanced Very High Resolution Radiometer (AVHRR) have been used to study vegetation through the use of indices and compositing procedures (Tucker, Gatlin, & Schneider, 1984). Data in the visible to middle infrared from the Thematic Mapper (TM) and the Multispectral Scanning Spectrometer on the Landsat series have been used for various applications in the land cover and land use community.

The MODIS instrument was designed building on the AVHRR and TM experience, to provide a global daily data set of very high radiometric and geometric quality in seven "land" bands (band 1: 648 nm at 250 m, band 2: 858 nm at 250 m, band 3: 470 nm at 500 m, band 4: 555 nm at 500 m, band 5: 1240 nm at 500 m, band 6: 1640 nm at 500 m, band 7: 2130 nm at 500 m). The bands were chosen carefully to minimize the impact of absorption by atmospheric gases (in particular water vapor) which has been a limitation of the previous instruments for land remote sensing (Vermote et al., 1997). Several advanced land products are now being generated using those bands: surface reflectance, VIs, LAI/FPAR, BRDF/Albedo, PSN/NPP, land use/land cover change and snow (Justice et al., 1998).

The surface reflectance product is defined as the reflectance that would be measured at the land surface if there were no atmosphere. It uses the MODIS L1B as the primary input and performs corrections for the effect of gaseous absorption, molecules and aerosol scattering, coupling between atmospheric and surface bi-directional reflectance function (BRDF) and adjacency effect (atmospheric point spread function). A detailed description of the algorithm has been provided in Vermote et al. (1997), and will not be represented in detail in this paper. In this paper, we focus on presenting the first results of the operational aerosol correction over land. Correction for aerosol effects constitutes a
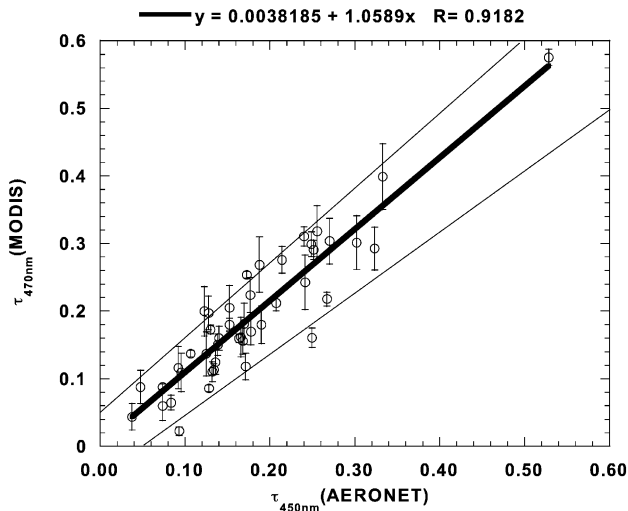
Fig. 1. Comparison of aerosol optical thickness retrieved by MODIS blue channel with AERONET Sun photometer measurements during the April 24, 2000 to June 10, 2000 period.

first and difficult step to obtaining the surface reflectance product. To our knowledge, these corrections have not been applied globally and consistently to any land data set on an operational basis. The operational correction of atmospheric effects has been limited to Rayleigh and ozone effects on the AVHRR Pathfinder data set (James & Kalluri, 1994). These first results obtained by MODIS show the bias in the signal introduced by aerosols even after a relatively long compo-

siting period (1 month) and therefore the importance of their correction prior to interpreting products derived from visible-near-infrared data.

## 2. Brief description of the surface reflectance algorithm

Molecular scattering, gaseous absorption and aerosols affect the top of the atmosphere (TOA) signal measured by the instrument. An atmospheric correction scheme based on the 6S radiative transfer code and accounting for the surface/atmosphere BRDF is used to compute the surface reflectance. A full description of the atmospheric correction process is included in the MODIS surface reflectance Algorithm Theoretical Basis Document (ATBD) (Vermote & Vermeulen, 1999) and in the paper describing the operational algorithm and its pre-launch validation (Vermote et al., 1997). This process can be approximated assuming a lambertian and uniform target, by the equation:

$$\rho_{TOA} = Tg(O_3, O_2, CO_2)\left[\rho_R + (\rho_{R+A} - \rho_R)Tg(U_{H_2O}/2)\right.$$

$$\left. + T_{R+A}\frac{\rho_s}{1 - \rho_s S_{R+A}}Tg(U_{H_2O})\right] \tag{1}$$

Where $\rho_{TOA}$ is the reflectance observed at the top of the atmosphere, Tg refers to gaseous transmission, $\rho_R$ is the molecular scattering intrinsic reflectance, $\rho_{R+A}$ is the intrinsic reflectance of the molecules and aerosols, $T_{R+A}$ is the transmission of the molecules and aerosols and $S_{R+A}$ is the
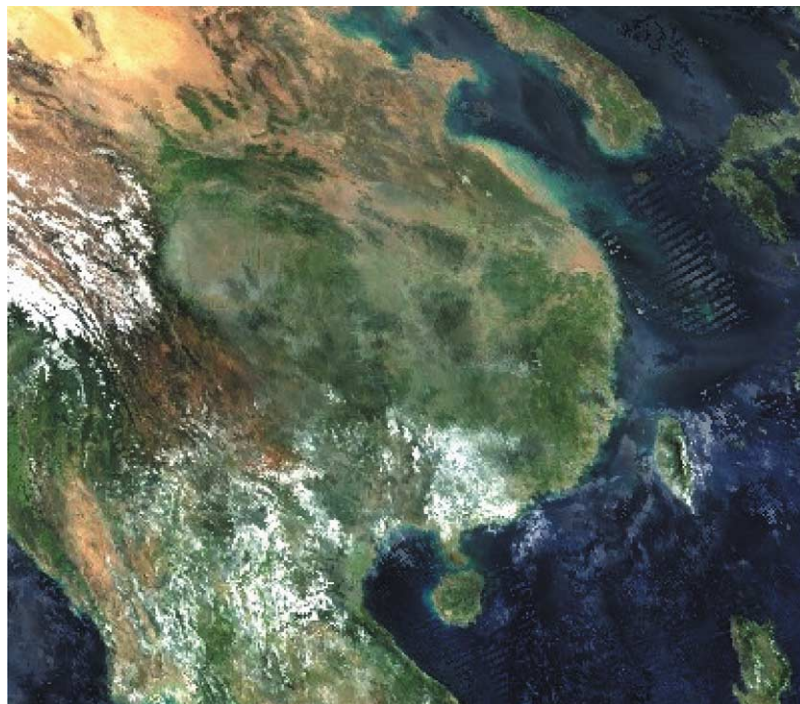


Fig. 2. RGB image of monthly composite surface reflectance not corrected for aerosol effect over China.
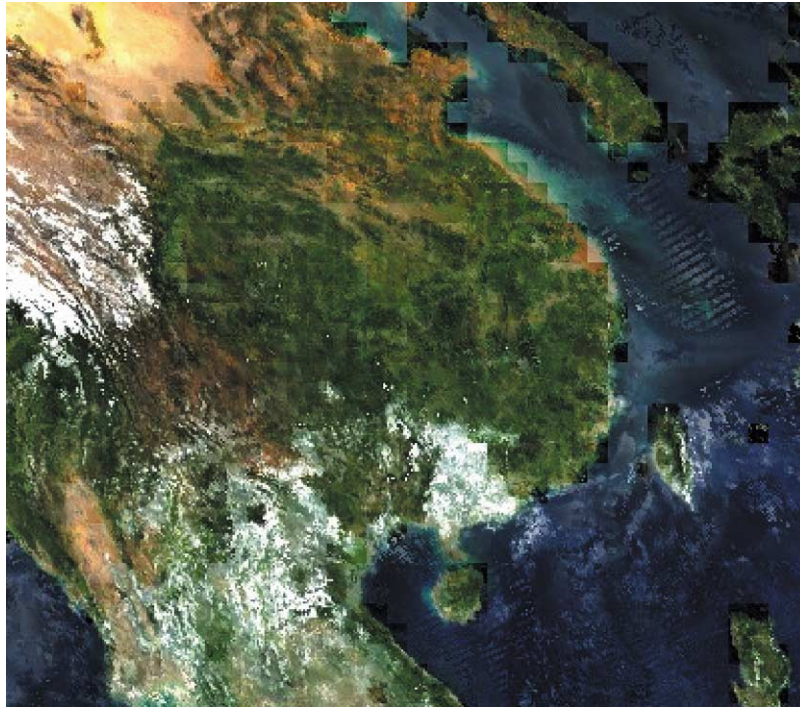
Fig. 3. RGB image of monthly composite surface reflectance *corrected* for aerosol effect over China.

spherical albedo. This equation accounts for the coupling between water vapor absorption and aerosol scattering in a simplified way (term in $U_{H_2}O/2$), which is of sufficient accuracy for MODIS where the absorption by water vapor in the visible and near-infrared bands is weak.

The atmospheric correction process currently relies on readily available ancillary data from National Centers for Environmental Prediction (NCEP) for the surface pressure, ozone and water vapor content inputs, but we are planning to use the MODIS water vapor product in the near future. Aerosol optical thickness (AOT) represents the most critical element in the correction scheme since it has a large effect on the visible and near-infrared bands and there is no readily available ancillary data that can provide this input. AOT is derived from MODIS data itself; the retrieval approach and limitations are described in the following sections.

## 3. MODIS at-launch aerosol algorithm results

The MODIS aerosol retrieval algorithm over land is fully described in Kaufman et al. (1997). The approach uses middle infrared bands (from 2.13 to 4.0 mic) where the aerosol effect is small, to predict the reflectance in bands where surface reflectance is small and the aerosol signal is strong, typically blue (450 nm) and red (650 nm) wavelengths. This method was successfully applied to a number of cases using AVHRR data (3.75 μm with 0.67 μm) and Thematic Mapper data (2.13 μm with 0.67 and 0.47 μm) (Ouaidrari & Vermote, 1999). Although some problems

have been encountered with this technique at very small optical depths ( ∼ 0.07) using Thematic Mapper (Wen, Tsay, Cahalan, and Oreopoulos, 1999), the approach is very
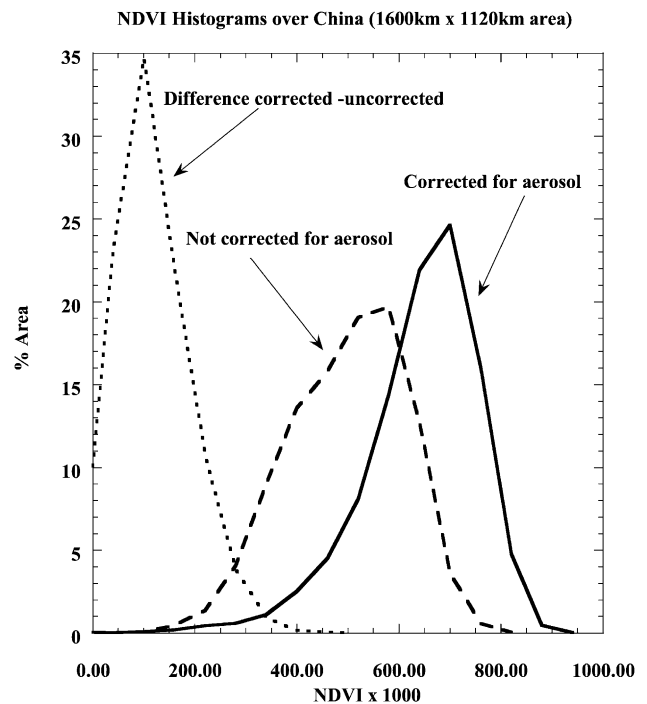


Fig. 4. Comparison of histograms of NDVI (corrected for aerosol and uncorrected for aerosol) observed over China (area of 1600 × 1120 km), the solid curve corresponds to the aerosol corrected data, the dashed one to the uncorrected and the small dash to the difference between uncorrected and corrected NDVI.

robust and has given excellent results with MODIS (Chu et al., in preparation). The MODIS aerosol product based on this algorithm is part of the suite of Atmosphere products run operationally in the MODIS Adaptive Processing System (Justice et al., 2002, this issue). Prior to using this product in the operational surface reflectance code, we conducted an evaluation at the Surface Reflectance Science Computing Facility (SCF).

Data collected from April 24, 2000 to May 23, 2000 were used to test the aerosol correction. First, the aerosol optical thickness was derived and the values screened for cloud-contaminated cases and unacceptably high spatial variability. The remaining data set was compared to the Level 1.5 (cloud screened) Aerosol Robotic Network (AERONET) data (Holben et al., 1998). Filtering was undertaken again based on temporal variability observed in the AERONET

data and time difference between AERONET measurements and MODIS retrieval ($\pm$ 30 min). Fig. 1 shows that the derived optical thickness compares extremely well with the measurements from AERONET. The error bars on the $Y$-axis represent the standard deviation of the MODIS retrieval. The two black lines are suggestive of the accuracy of the product ($0.05 \pm 0.1\tau$) which is actually much better than the accuracy predicted prior to launch ($0.05 \pm 0.2\tau$).

The results of the aerosol correction on the test data set are illustrated focusing on an area over China by Figs. 2 and 3, which are red, green, blue (RGB) images of the monthly composite of the surface reflectance data, composited using minimum band 3. The aerosol corrected version shows enhancement of the signal and improvements following aerosol correction. The quality of these images is far from perfect, since the inputs used were coarse resolution 5-km
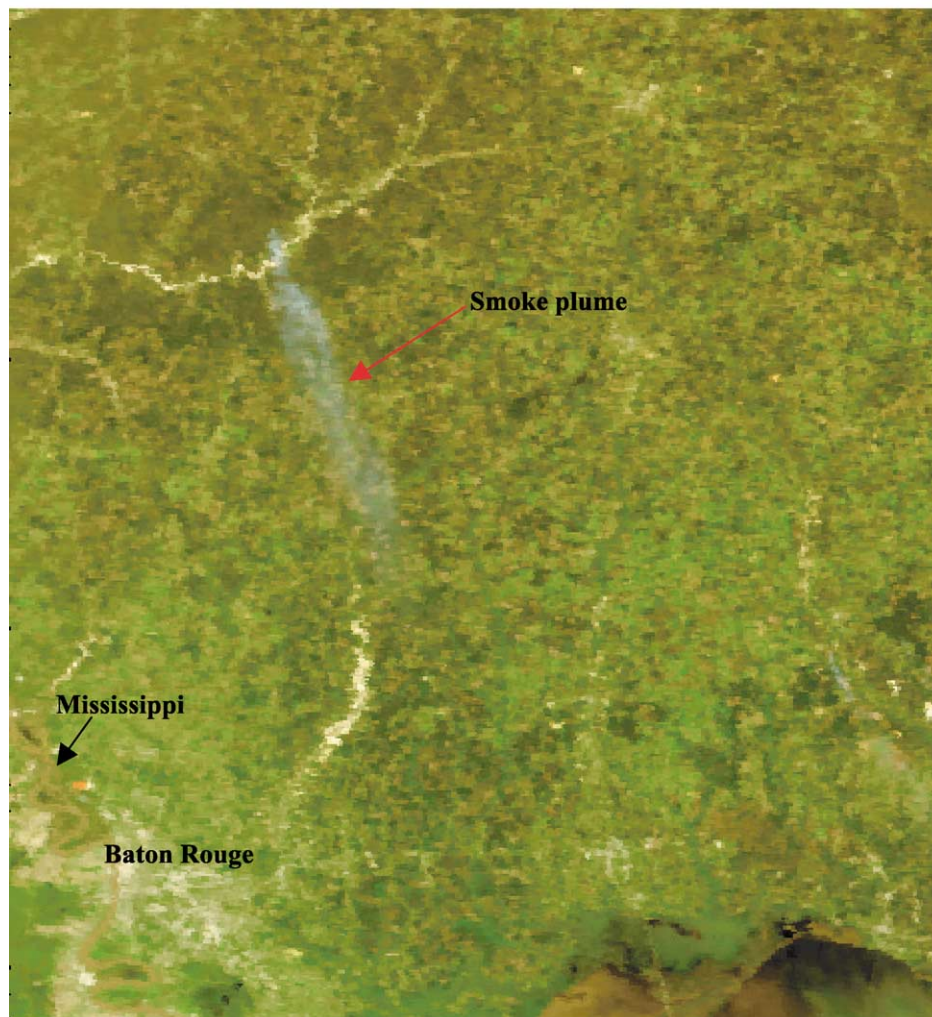
**(a)**



Fig. 5. (a) RGB image of 500-m resolution data (not corrected for aerosol effect) collected by MODIS over Louisiana on March 21, 2001 at 16:50 GMT. Note the smoke plume indicated by the red arrow. (b) Same as (a) but this time, the 1-km aerosol correction has been applied. The smoke plume disappeared except for area near the smoke source due to the extreme variability of the AOT near the source and the fact that the aerosol optical thickness cannot be reliably retrieved over the fire itself. (c) Aerosol optical depth at 470 nm corresponding to the area of (a). (d) False RGB (R = 3.75 μm, G = 1.6 μm, B = 2.13 μm) of the area of Louisiana presented in (a)–(c) showing the presence of several active fires (small red clusters, indicated by red arrows) in particular two larger clusters at the location of the smoke sources as identified by the aerosol product.

(b)



Fig. 5 (*continued*).

data and the prototype 50-km aerosol product, resulting in a blocky appearance to the corrected image. However, it clearly demonstrates the effectiveness of the aerosol correction. This aerosol perturbation is important and will adversely effect the interpretation of the land surface products if not accounted for. Fig. 4 shows the histograms of the NDVI for China with (solid curve) and without (dashed curve) aerosol correction and the histogram of the difference between the two NDVIs (small dashed curve). Differences greater than 0.10 NDVI units can be observed on this monthly composite for about 75% of the pixels, over an NDVI range of 0.4–0.9.

## 4. Development of an improved MODIS aerosol correction

The MODIS aerosol correction was put in operation for data acquired after Julian day 273, 2000. Globally, it performed well, and improved the accuracy in the downstream products, in particular the BRDF/Albedo product suite. Two problems were identified with this product, namely the sensitivity to snow which was sometimes confused with dark targets, since it has a low reflectance in the middle infrared, and the limitation of the retrieval to targets of less than 0.15 reflectance in the middle infrared (or 0.035 at 470 nm). A new version of the aerosol algorithm was developed to address those issues. In addition to filtering-out snow and extending the retrieval to brighter targets, we also retrieved the aerosol at a much higher spatial resolution (1 km) than the at-launch version (18 km) which enabled correction of small, discrete aerosol features such as smoke plumes.

Fig. 5a–c illustrates the new 1-km aerosol product used in the correction for an area where some fires were active and producing smoke. Fig. 5a, which was not corrected for aerosols, shows a large smoke plume indicated by red arrow. In Fig. 5b, which was corrected for aerosol, the smoke
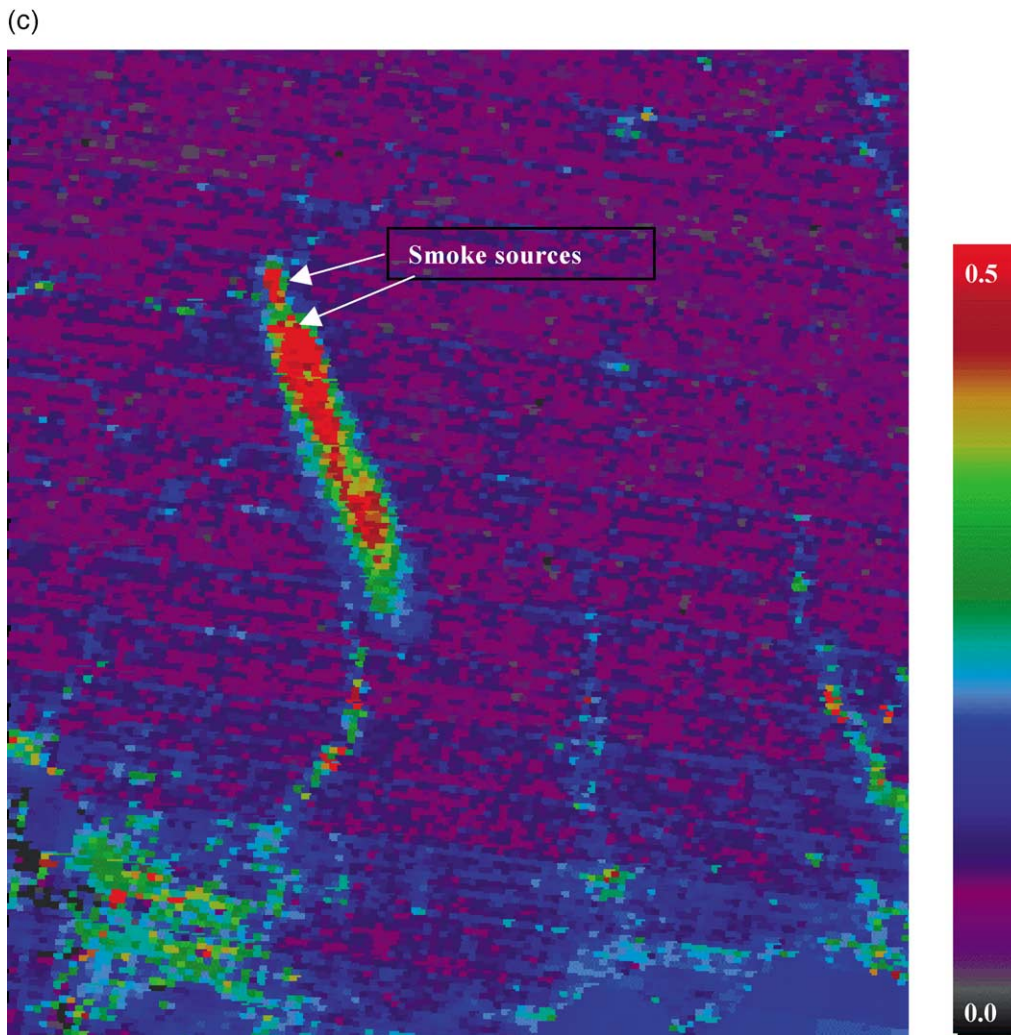
(c)



Fig. 5 (*continued*).

plumes disappears and the image shows no evidence of under or over-correction. There is some residual smoke contamination in the vicinity of the smoke source, due to the very high heterogeneity of the aerosols near the source and the fact that the aerosols cannot be inverted in a reliable way over fire since they may perturb the 2.13 μm signal. Fig. 5c shows the aerosol optical thickness and the higher values for the smoke plume and also evidence of two distinct sources of smoke. By looking at the thermal anomalies RGB (R = 3.75 μm, G = 1.6 μm, B = 2.13 μm; see Petitcolin & Vermote, 2002, this issue, for details) presented in Fig. 5d, one can actually locate two clusters of active fires associated with the two smoke plumes.

New tests have also been added to filter snow pixels or partially filled snow pixels prior to the derivation of the optical thickness. Fig. 6a–c illustrates the problem we encountered with the at-launch aerosol algorithm. Fig. 6a shows an RGB image of MODIS data, not corrected for

aerosol, of the southwest United States and Mexico. Some snow is present in higher elevation areas as indicated by the red arrows. Fig. 6b shows again the MODIS RGB data, but this time corrected for aerosols using the at-launch version of the aerosol retrieval algorithm. Areas near snow are over-corrected and even saturated at − 0.01 reflectance unit. Fig. 6c shows the MODIS RGB data corrected using the new algorithm, which uses additional criteria to filter out snow prior to derivation of optical thickness. One can easily see that the artifact present in the at-launch version has disappeared. The filtering of snow relies on using band 5 (1.24 μm) in addition to the usual snow mask. A very conservative test is applied, using the ratio of bands 5 to 2 (1.24 μm/0.87 μm). Snow or cloud will decrease the value of that ratio whereas snow-free land surface will have a ratio of greater than one. This suggested approach to filter-out such cases has been communicated to the MODIS Aerosol team and they are
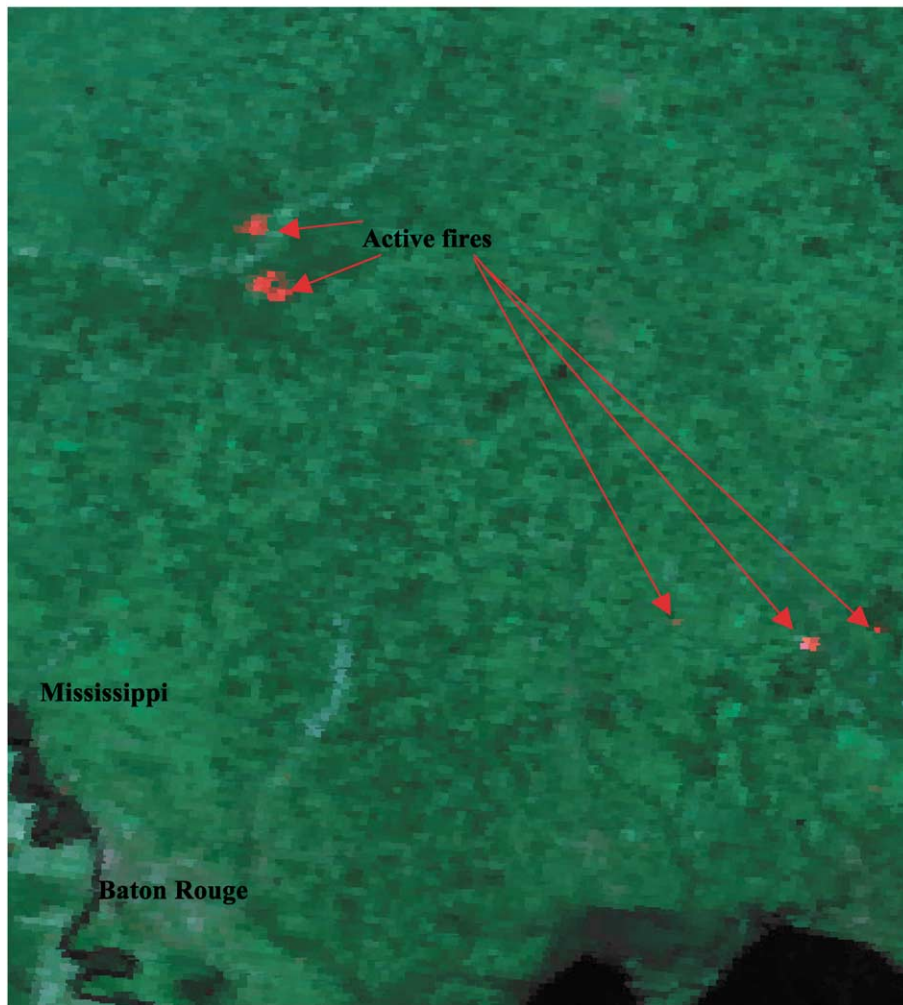
(d)



Fig. 5 (*continued*).

conducting their own evaluation prior to adopting it in the operational aerosol algorithm.

One other important area of improvement is the extension of the aerosol retrieval to targets of reflectance brighter than 0.035 at 0.47 μm. This improvement is illustrated by the figure showing the RGB uncorrected for aerosol (Fig. 7a), the RGB corrected for aerosol (Fig. 7b) and the aerosol optical thickness used in the correction (Fig. 7c). One can see that no visible artifacts were introduced by the correction. The relationship used to predict the reflectance at 0.47 μm is not solely based on the 2.13-mic channel, but is computed for sparsely vegetated areas from the value of a ratio using bands 2 (0.87 μm) and 5 (1.24 μm). Sparsely vegetated bright areas are identified using an index that combines bands 6 (1.6 μm) and 7 (2.13 μm), which is insensitive to most aerosol types. This relationship was tested on several AERONET sites, where surface reflectance was computed using aerosol optical thickness derived from the sun photo-meter measurements. Fig. 8 shows a comparison of predicted and observed reflectance.

Optical thickness derived using the new aerosol algorithm was compared to the AERONET measurements for selected cases over a period of 3 months (Fig. 9). The values compare very well especially at low optical thickness, which is important for an operational atmospheric correction algorithm.
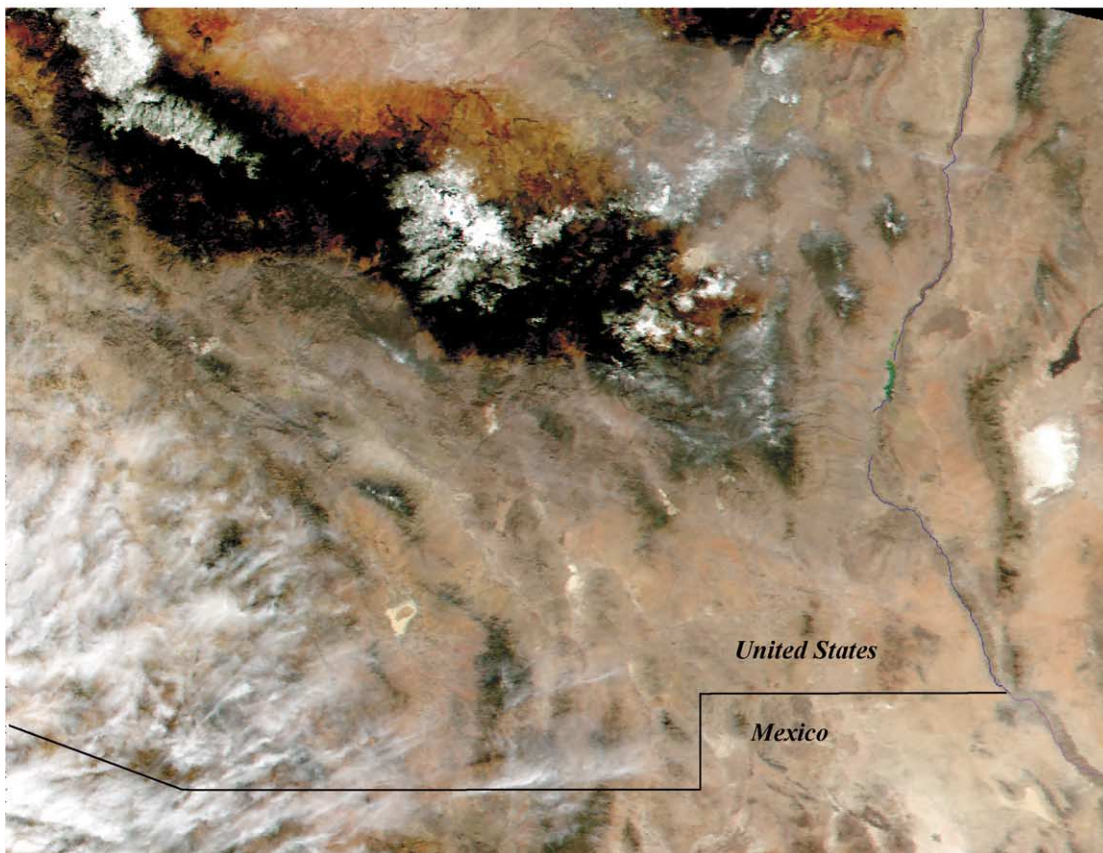
## 5. Preliminary validation of the MODIS surface reflectance

MODIS surface reflectance was evaluated by comparing it with Landsat 7 Enhanced Thematic Mapper (ETM+) data. We used AERONET water vapor (2.15 cm) and aerosol (0.12 at 550 nm) obtained from the AERONET web site (http://aeronet.gsfc.nasa.gov:8080/), and atmospheric cor-
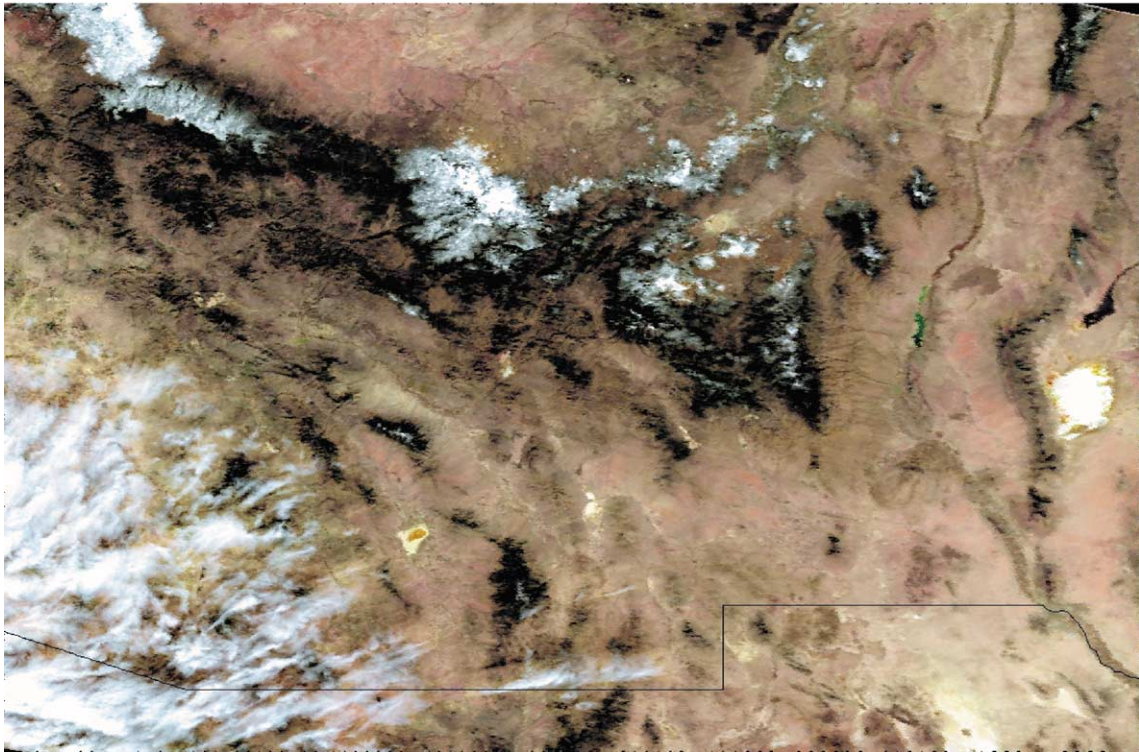
(a)
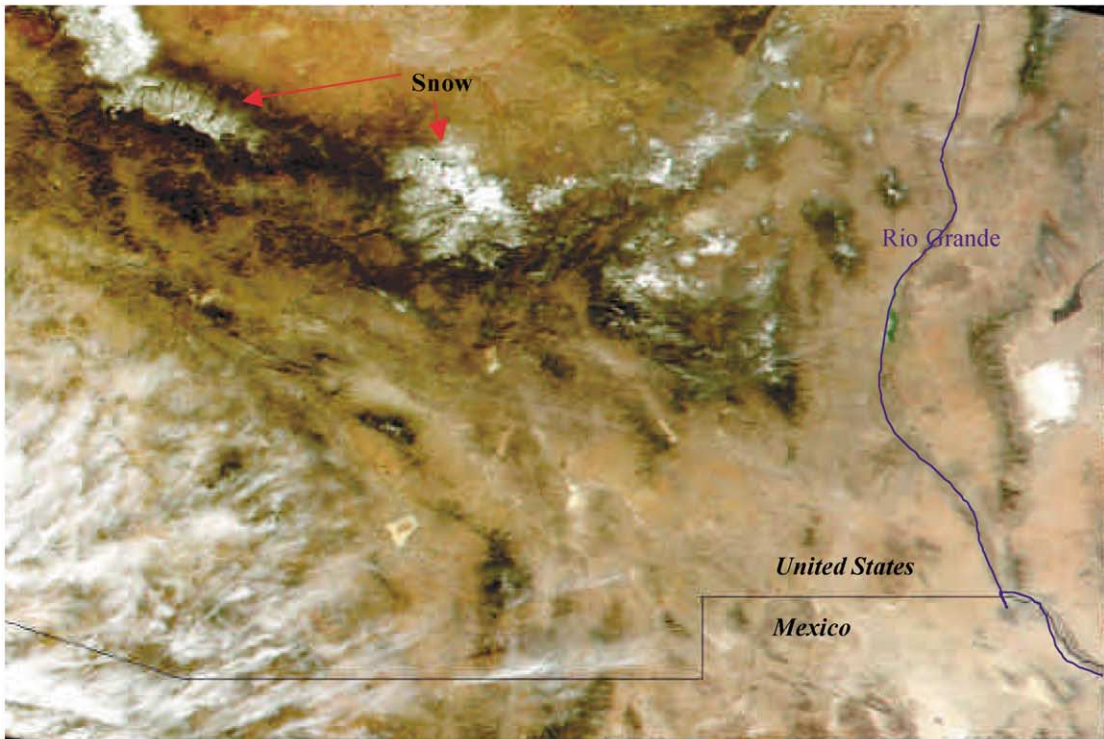


(b)

(c)



Fig. 6. (a) RGB image of MODIS data, not corrected for aerosol, of the southwest United States and Mexico, some snow is present in higher elevation areas as indicated by the arrows. (b) RGB image of MODIS data over the same area as (a) but corrected for aerosol using the at-launch version of the aerosol retrieval algorithm, areas near snow are over-corrected and even saturated at − 0.01 reflectance unit. (c) Same as (b) but this time, the data are corrected using the new version of the aerosol retrieval algorithm that aggressively filters out snow pixels.

rection code for Landsat Thematic Mapper described in Ouaidrari and Vermote (1999). Prior to comparison, rigorous cloud screening was performed in both data sets. We also filtered Thematic Mapper data to select spectrally uniform areas of $10 \times 10$ 30-m pixels for comparison with the MODIS 250-m data and $20 \times 20$ 30-m pixels for comparison with 500-m MODIS data. Areas were selected with a standard deviation under 10–20%, depending on the band. Fig. 10 shows the comparison between the two data sets for a uniform area located on the Thematic Mapper image of $21 \times 18$ km. The correlation between the two data sets is high due to the fact that we eliminated most of the uncertainty in the MODIS sub-pixel scale by the standard deviation filtering. The dynamic range of the land reflectance is very well represented by the selected sample. The two data sets compare extremely well both in terms of standard deviation and slope for most bands (note band 5 is not present on ETM+). The differences observed are well within the range of the expected accuracy of the MODIS surface reflectance (Vermote & Vermeulen, 1999), except for the 2.13-μm band. Differences between MODIS and ETM+ could be attributed not only to uncertainty in the atmospheric correction but also to differences in the spectral

bands and also to calibration uncertainties, both of which need to be investigated further.

The reflectance obtained from ETM+, including correction for the adjacency effect, was compared to field measurements taken with an Analytical Spectral Devices (ASD) spectrometer at the United States Department of Agriculture (USDA), Beltsville Agricultural Research Center. The spectra were averaged and integrated over the ETM+ spectral band to provide validation of the ETM+ atmospherically corrected reflectance and therefore indirectly the MODIS surface reflectance. Measurements were collected at three different locations (bare soil, yellow grass, and a harvested corn field). Fig. 11a–c shows the comparison between the surface measurements and the ETM+ surface reflectance as a function of the central wavelength of each ETM+ band (0.47, 0.55, 0.67, 0.87, 1.6, 2.13 μm). The error bars on the ASD measurements represent the standard deviation computed from the spectra collected at the location (about 30 measurements).

The harvested corn site gives the best results, probably because it is the largest uniform area ($120 \times 250$ m) of the three locations and also because the ASD measurements show a very good uniformity at ETM+ sub-pixel levels (low

standard deviation). Each ASD measurement corresponds to surface area of 0.5 m in diameter. The grass site and the soil site correspond only to a few ETM+ pixels (30 × 30 m each). The soil site shows very high non-uniformity at the

ETM+ sub-pixel level but the ETM+ reflectances are still within 1 standard deviation of the mean ASD reflectance. Based on this limited data set, we can say that the ETM+ corrected reflectance compares very well with the ground

**(a)**



Fig. 7. (a) RGB image of MODIS data (not corrected for aerosol) over South Africa acquired on September 13, 2001 between 08:45 and 08:50 GMT. (b) Same as (a), but this time, aerosol correction has been applied. (c) Aerosol optical thickness at 0.67 μm corresponding to the data of (a), the water bodies are outlined in white and the clouds are masked in magenta.
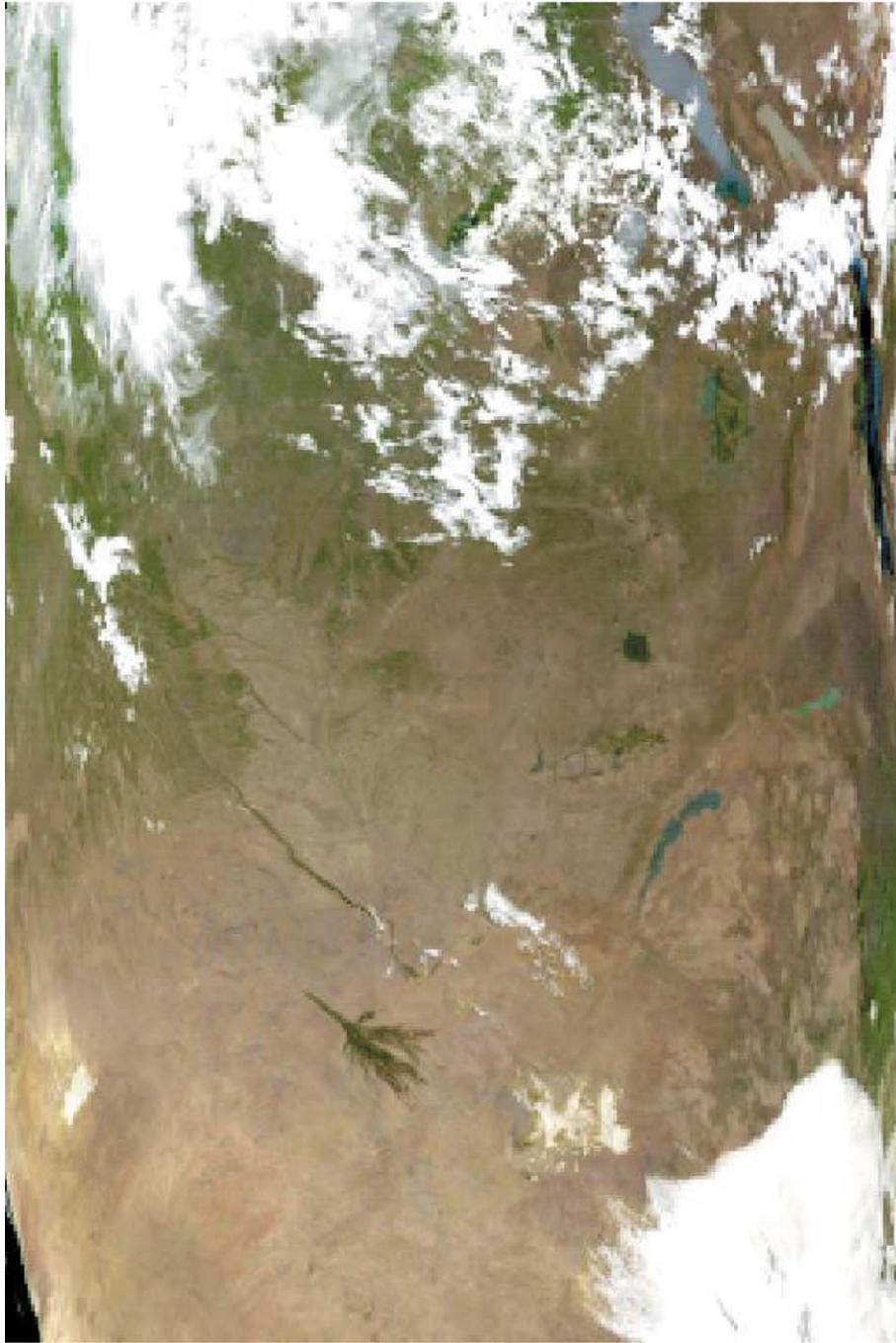
(b)



Fig. 7 (*continued*).

measurements and exhibits no bias due to atmospheric correction and therefore can be used to indirectly "validate" the MODIS reflectance product.

We also used this limited data set to examine the differences in spectral response between MODIS and ETM+ bands. Fig. 12 compares the reflectance integrated over MODIS versus ETM+ bands for the three different sites. The largest difference can be observed in band 3 (0.47 μm),

where MODIS surface reflectance is about 7% lower than the corresponding ETM+ band 1. This explains some of the differences observed at 0.47 μm in Fig. 10 (13% difference) where for most surfaces, there is a decrease in reflectance in the blue. A systematic adjustment between ETM+ band 1 and MODIS band 3 needs to be taken into account when comparing both data sets. However, the difference of 12% observed between ETM+ band 7 and MODIS band 7 could
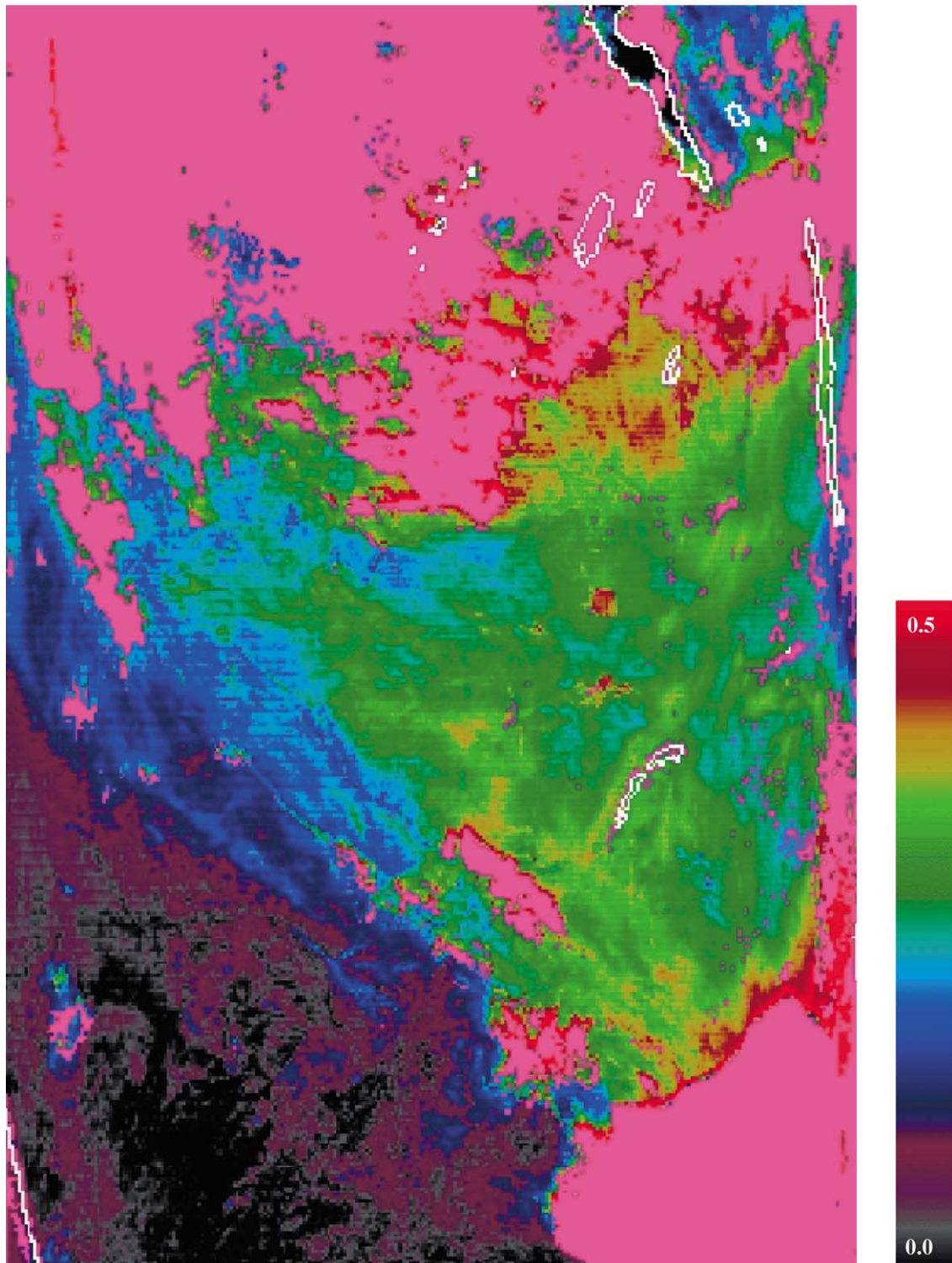
(c)



Fig. 7 (*continued*).

not be explained by this data set. The high standard deviation observed in the ASD measurements for that band and the limited scope of our validation data set prevent any con-clusive analysis and further investigation is needed. The values of the middle infrared bands could be used to determine if the field measurements performed at a site are
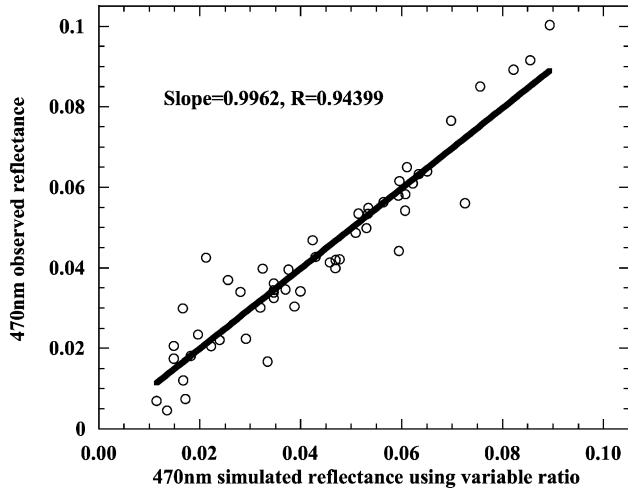
Fig. 8. Comparison of the simulated 0.47-μm surface reflectance (X-axis) with the actual reflectance (Y-axis) over selected validation sites.



Fig. 10. Comparison of the surface reflectance derived from ETM+ (using AERONET data) with the operational MODIS surface reflectance product.

representative of the ETM+ pixel as these bands are only slightly affected by the atmosphere, mainly just in the gaseous transmission in which one should be able to compute accurately to within 2–3%. For example, if the average ASD reflectance in those bands does not match the ETM+ measurements, then there is a strong indication that the site has not been characterized properly or is too variable at the pixel level.

In the future, we intend to apply the approach we have taken with ETM+ in a more systematic way: (1) we derive ETM+ surface reflectance using atmospheric correction and Sun photometer measurements and ancillary data for atmos-
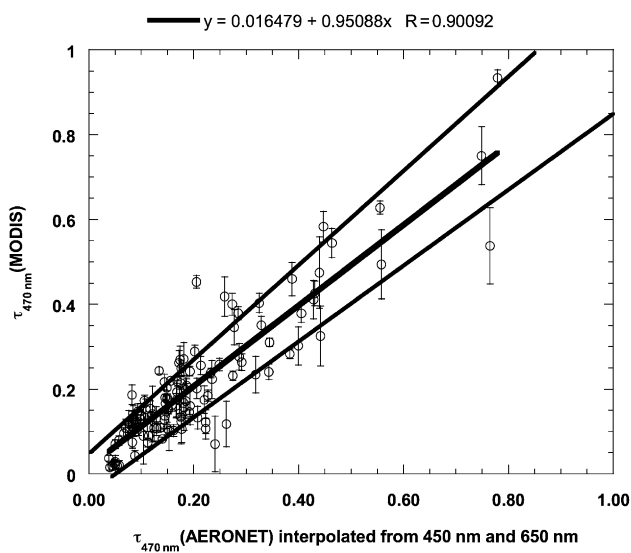
pheric parameters, (2) we validate ETM+ reflectance at specific locations using ASD reflectance measurements, (3) we compare MODIS surface reflectance to averaged ETM+ surface reflectance over uniform areas. This strategy could be applied to ASTER data to extend the validation to off-nadir observations.

## 6. Conclusion

The first results obtained with the MODIS reflectance product indicate that the aerosol retrieval and correction techniques are effective and can be applied on an operational basis. They also show that the impact of aerosols on visible and near-infrared reflectances or a combination of those bands (e.g. NDVI) is very important, and that aerosol effects remain in uncorrected data sets even after long compositing periods (e.g. a month).

The aerosol retrieval algorithm has been refined and extended to more cases , including semi-arid surfaces and at higher spatial resolutions. Some of the incorrect retrievals, e.g. for snow, can be eliminated through better screening prior to aerosol inversion. This new version of the algorithm should improve further the quality of the reflectance product particularly at the global scale and in "difficult cases" (e.g. smoke plumes) and where there is a high spatial variability in the aerosol layer.

At this time, preliminary validation indicates that the product is well within the error bars announced in the ATBD. This preliminary validation has enabled us to devise specific validation techniques that can be applied in a more systematic way. The next step in the refinement of the MODIS surface reflectance product is to implement correction for both adjacency effects and atmosphere surface



Fig. 9. Comparison of 1-km operational aerosol optical thickness retrieved by MODIS blue channel ( ∼ 120 matches) with AERONET sun photometer measurements during the March, April, May 2001 period.
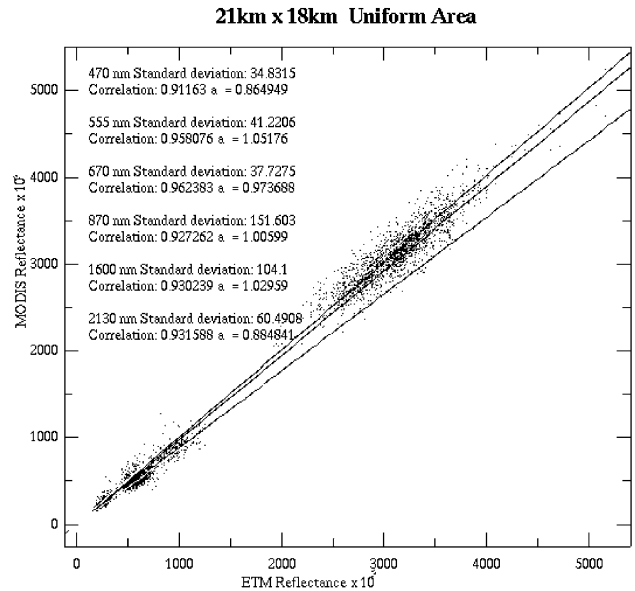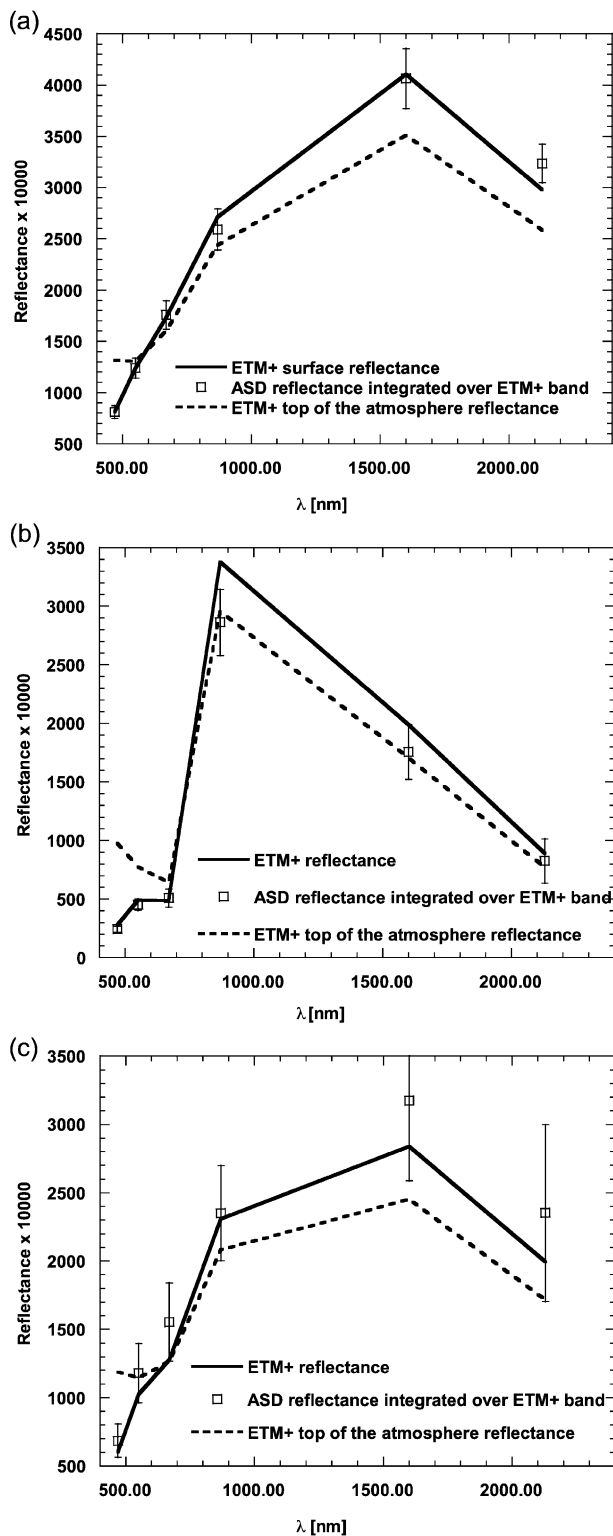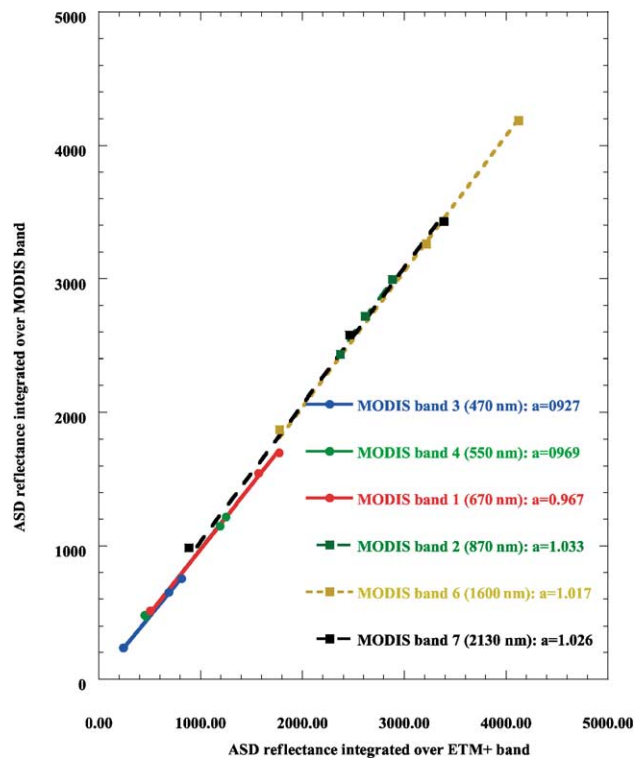
Fig. 12. Comparison of reflectance from the ASD measurements integrated over MODIS band versus integrated over ETM+ band for the soil, grass and harvested corn plots.

BRDF coupling, and their impacts on the aerosol retrieval, which present an interesting challenge both in terms of operational implementation and validation. High spatial resolution data such as ETM+ or ASTER will be critical to evaluate the adjacency effect correction and MISR/ASTER and MODIS PM data will be useful to address angular effects.

## Acknowledgements

## References

Chu, D. A., Kaufman, Y. J., Ichoku, C., Remer, L., Tanre, D., & Holben, B. N. (2002). Validation of the MODIS aerosol retrieval over land. *Geophys. Res. Lett.*, *29*(12), 1–4 (MOD 2).

Holben, B. N., Eck, T. F., Slutsker, I., Tanre, D., Buis, J. P., Setzer, A., Vermote, E., Reagan, J. A., Kaufman, Y., Nakajima, T., Lavenu, F., Jankowiak, I., & Smirnov, A. (1998). AERONET—a federated instrument network and data archive for aerosol characterization. *Remote Sensing of Environment*, *66*, 1–16.

James, M. E., & Kalluri, S. N. V. (1994). The Pathfinder AVHRR land data



Fig. 11. (a) Comparison of the ETM+ surface reflectance with ground measurements (ASD) for the harvested corn plot. (b) Comparison of the ETM+ surface reflectance with ground measurements (ASD) for the yellow grass plot. (c) Comparison of the ETM+ surface reflectance with ground measurements (ASD) for the soil plot.

set—an improved coarse resolution data set for terrestrial monitoring. *International Journal of Remote Sensing, 15*(17), 3347–3363.

Justice, C. O., Townshend, J. R. G., Vermote, E., Wolfe, R., El Saleous, N., & Roy, D. (2002). Status of MODIS, its data processing and products for terrestrial science applications. *Remote Sensing of Environment, 83,* 3–15 (this issue).

Justice, C. O., Vermote, E., Townshend, J. R. G., Defries, R., Roy, D. P., Hall, D. K., Salomonson, V. V., Privette, J. L., Riggs, G., Strahler, A., Lucht, W., Myneni, R. B., Knyazikhin, Y., Running, S. W., Nemani, R. R., Wan, Z. M., Huete, A. R., van Leeuwen, W., Wolfe, R. E., Giglio, L., Muller, J. P., Lewis, P., & Barnsley, M. J. (1998). The Moderate Resolution Imaging Spectroradiometer (MODIS): land remote sensing for global change research. *IEEE Transactions on Geoscience and Remote Sensing, 36*(4), 1228–1249.

Kaufman, Y. J., Tanre, D., Remer, L. A., Vermote, E. F., Chu, A., & Holben, B. N. (1997). Operational remote sensing of tropospheric aerosol over land from EOS moderate resolution imaging spectroradiometer. *Journal of Geophysical Research-Atmosphere, 102*(D14), 17051–17067.

Ouaidrari, H., & Vermote, E. F. (1999). Operational atmospheric correction of Landsat TM data. *Remote Sensing of Environment, 70*(1), 4–15.

Petitcolin, F., & Vermote, E. (2002). Land surface reflectance, emissivity and temperature from MODIS middle and thermal infrared data. *Remote Sensing of Evironment, 83,* 112–134 (this issue).

Tucker, C. J., Gatlin, J. A., & Schneider, S. R. (1984). Monitoring vegetation in the Nile delta with NOAA-6 and NOAA-7 AVHRR imagery. *Photogrammetric Engineering and Remote Sensing, 50*(1), 53–61.

Vermote, E. F., El Saleous, N. Z., Justice, C. O., Kaufman, Y. J., Privette, J. L., Remer, L., Roger, J. C., & Tanre, D. (1997). Atmospheric correction of visible to middle-infrared EOS-MODIS data over land surfaces: background, operational algorithm and validation. *Journal of Geophysical Research-Atmosphere, 102*(D14), 17131–17141.

Vermote, E. F., Vermeulen, A. (1999). Atmospheric correction algorithm: spectral reflectances (MOD09). AlgorithmTheoretical Background Document available on line at http://modarch.gsfc.nasa.gov/MODIS/ATBD/atbd_mod08.pdf.

Wen, G. Y., Tsay, S. C., Cahalan, R. F., & Oreopoulos, L. (1999). Path radiance technique for retrieving aerosol optical thickness over land. *Journal of Geophysical Research-Atmosphere, 104*(D24), 31321–31332.